Development of an Automatic Perturbator for Dynamic Posturographic Analysis

Development of an automatic perturbator for dynamic posturographic analysis

Carlo Ferraresi[1][0000-0002-9703-9395], Carlo De Benedictis[1][0000-0003-0687-0739], Giovanni Gerardo Muscolo[1][0000-0002-3248-5888], Oliviero Walter Pica[1], Marco Genovese[1], Daniela Maffiodo[1][0000-0002-5831-8156], Walter Franco[1][0000-0002-0783-6308], Maria Paterna[1], Silvestro Roatta[2][0000-0001-7370-2271], Zeevi Dvir[3]

[1] Department of Mechanical and Aerospace Engineering, Politecnico di Torino, Italy
[2] Department of Neuroscience, University of Torino, Italy
[3] Department of Physical Therapy, Tel Aviv University, Tel Aviv, Israel
carlo.debenedictis@polito.it

Abstract. The subject of this paper is a novel pneumo-tronic system aimed at applying impulsive force perturbations to the human body in order to elicit postural reactions. The development of the prototype is based on the use of a specifically realized experimental test bench. An analytical model of the whole system, including its interaction with both the subject's body and with the operator, is briefly presented. The test bench is used to validate the model and to perform experimental trials. The results confirm the validity of the model but call for a more accurate selection of the system components and of the control logic, in order to achieve the desired performance for such a demanding application.

Keywords: Pneumo-tronics, Force impulse control, Posturography, Human balance.

1 Introduction

The ability to maintain balance is a fundamental skill for human beings, necessary for the correct execution of basic life activities. The alteration of the human balance control due to trauma or diseases can be dangerous since it is related to an increased risk of falls, which can lead to an overall reduction in quality of life. For these reasons, it may be necessary to assess quantitatively the ability to keep or regain balance when one is subjected to an external perturbation (e.g. mechanical, visual or vestibular) [1]. This assessment aims at eliciting the so-called postural reactions (PR), a set of coordinated movements of body segments intended to return the body to the pre-perturbation status. PR can typically be analyzed by considering the excursion of the Center of Pressure (CoP), the instantaneous mean of the ground reaction force vectors defined relative to the Base of Support (BoS) [2–4], the activation of specific muscles devoted to the control of balance (measured by surface electromyography, sEMG) [2, 5], or by the increase in body sway [6, 7]. The multiplicity of stimulations available is related to the complexity of the human balance control system, which comprises the

visual [8], vestibular [9, 10] and proprioceptive [11] systems. All inputs from these systems are integrated by the Central Nervous System (CNS) which develops the required action to maintain balance [12, 13] by coordinating the activity of different muscle groups according to different motor strategies (ankle, hip, step).

Many systems described in the literature apply perturbation to the human body by shifting and/or tilting of the BoS [2, 3, 14], which can be accomplished quite accurately by means of linear motors or even more complex solutions such as a Stewart platform [15]. In other studies, mechanical perturbations were imparted using cables and pulleys [4, 16, 17] which were used to connect the body to one or multiple suspended weights, or by a pendulum-like structure impacting the subject [18, 19]. The existing systems often share the same limitations, in terms of scalability and adaptability of the perturbation. The scalability is the possibility to change the magnitude of the perturbation with respect to the characteristics of a specific individual e.g. his health condition, anthropometry, age etc. The adaptability is related to the ability of the system to modify such perturbations according to variable conditions such as different points of application, directions and timing of stimuli.

The objective of our research was to realize a novel automatic device intended for the application of controllable, scalable and adaptable perturbations to the human body for the analysis of PR. The device had to be sufficiently robust to compensate for the uncertainties deriving from the behavior of the operator and the subject under examination. A first prototype has previously been described in [20], reporting some preliminary results of experimental trials and highlighting several limitations and critical aspects of the device. The current work presents an analytical model of the whole system and an experimental bench that includes the mechanical impedances of the tester who handles the device and that of the target subject.

2 Materials and methods

Figure 1 shows two possible versions of a perturbation device: a manual (MP) and an automatic (AP). The MP (Fig. 1 left) is actuated directly by the operator. It is made up of a handle, grasped by the operator, a soft end pad for interaction with the patient, and a load cell for evaluating the contact force. With this solution, the perturbation is fully determined by the action of the operator. The AP (Fig. 1, right) is designed as an automatic system, able to control in real time the perturbation. In this case, the operator, who maneuvers the device by means of two handles, is only required to bring the perturbator proximal to the subject at given position and orientation, and then to activate it by a trigger; the characteristic of the perturbation is automatically controlled by the perturbator itself. The device is made up of a double acting pneumatic cylinder, whose rod ends with a load cell and a soft pad for contacting the patient's body. The motion of the piston, as well as the force exerted to the subject, are controlled by regulating the air flow to the cylinder chambers by means of two electro-pneumatic flow-proportional valves. In order to optimize the overall dynamics, the valves are located close to the actuator. All main components are detailed in Table 1. The real time control of the perturbator is implemented on an acquisition/control system (dSPACE®,

Paderborn, Germany) equipped with an analog/digital board A/D DS2002 for signal acquisition and a digital/analog board D/A DS2001 for valve regulation. The control system is programmed in MATLAB® Simulink® (The MathWorks, Inc., Natick, Massachusetts, USA) using ControlDesk® (dSPACE®, Paderborn, Germany) application.

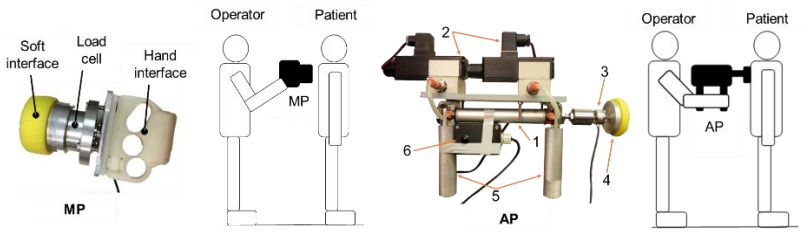

Fig. 1. Manual (MP, left) and Automatic (AP, right) Perturbator**.**

Table 1. Components of the Automatic Perturbator (AP).

Item	Details
1	Double acting cylinder ISO 6432 (Metal Work S.p.A., Concesio, Italy), diameter 25 mm, stroke 120 mm
2	Flow proportional valves 3AF2 (CKD Corporation, Komaki, Japan), analog input 0-10 V
3	Uniaxial load cell, UMM, range 50 kgf (DACELL Co., Ltd, Cheongwon-gun, Korea)
4	End damping pad with a 20mm thick layer of synthetic material (polyethylene)
5	Handles (aluminum)
6	Trigger

The AP was intended to automatically control the perturbation imparted to the subject, according to a predetermined pattern. A preliminary study on healthy subjects conducted with the MP highlighted an almost linear correlation between the displacement of a subject's CoP (detected by a force platform) and the impulse of the perturbation (i.e. the time integral of the contact force), rather than the intensity of the force itself. Based on this study, we selected, as a significant perturbation, a force impulse of 50 N amplitude with a duration of 250-500 ms. Therefore, we decided to realize an experimental bench (Fig. 2) aimed at: (i) verifying the actual behavior of the AP prototype; (ii) identifying all hardware and software requirements to achieve the desired performance. Since the AP interacts with two individuals, i.e. the operator and the tested subject, the experimental bench was conceived with the aim of replicating these actual operating conditions. The AP was placed on a cart sliding on a low friction linear guide. Such motion is constrained by a custom visco-elastic damper representing the interaction between the AP and the operator. On the other side, a mass placed on a second cart is in turn connected to a visco-elastic damper partially restraining its motion. This part of the test bench represents the mechanical impedance of the subject's body. In this way, only the passive response of the subject is considered whereas the active neuro-muscular response is neglected. To monitor con-

tact force, cart's displacement and actuator stroke, proper sensors have been installed (Fig. 2).

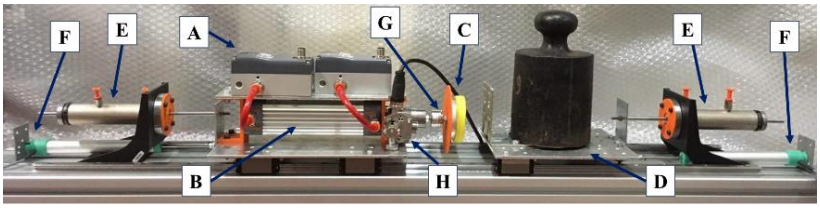

Fig. 2. The test bench: A: valves; B: cylinder; C: end damping pad; D: stricken body; E: dampers; F: potentiometers; G: load cell; H: laser distance sensor.

An analytical model comprising all elements of the AP and of the test bench, whose scheme is demonstrated in Fig. 3, has been developed to study the behavior of the system. It includes a pneumatic cylinder with mass M_1 controlled by two valves (V_a and V_b). The compliance of the operator is reproduced by a Kelvin-Voigt model with constants k_1 e β_1; M_2 can be considered as the equivalent mass of the subject and his interaction with the environment is reproduced with a second compliance (k_2 e β_2). A third compliance in the model is set to deal with the interaction between the AP and the subject (k_3 e β_3). The continuity equations (1) and (2) describe the evolution of the pressure in the pneumatic actuator, while equation (3) represents the dynamic equilibrium of the piston:

$$\frac{dP_r}{dt} = \frac{G_r n R T_{r_i}}{A_r (x_0 + x_{r_m} + x_3)\left(P_r / P_{r_i}\right)^{\frac{1}{n}-1}} - \frac{P_r n}{(x_0 + x_{r_m} + x_3)} \frac{dx_3}{dt} \tag{1}$$

$$\frac{dP_f}{dt} = \frac{G_f n R T_{f_i}}{A_f (x_0 + x_{f_m} - x_3)\left(P_f / P_{f_i}\right)^{\frac{1}{n}-1}} + \frac{P_f n}{(x_0 + x_{f_m} - x_3)} \frac{dx_3}{dt} \tag{2}$$

$$m\left(\frac{d^2 x_3}{dt^2} + \frac{d^2 x_1}{dt^2}\right) + F_e + p_f A_f - p_r A_r + F_{fr} \cdot \mathrm{sgn}\left(\frac{dx_3}{dt}\right) = 0 \tag{3}$$

The subscripts *r* and *f* refer respectively to the rear and front chamber of the cylinder, P is the absolute pressure in each chamber, P_i is the absolute initial pressure, p is the relative pressure in each chamber, G is the air mass flow rate, A is the piston section, x_0 is half stroke of the cylinder, x_m is the chamber dead band of the cylinder, T_i is the initial chamber temperature, n is the air polytrophic coefficient, R is the air constant and x_3 is the relative position of the piston rod (with respect to the cylinder frame). In Eq. (3), x_1 is the displacement of the cylinder frame, hence $x_1 + x_3$ is equal to the absolute positioning of the piston rod. F_e is the external force acting on the piston rod, given by the contact between the perturbator and the subject, whereas F_{fr} is the piston friction force. The dynamic behaviors of the cylinder frame and of the stricken body are respectively described in Eqs. (4) and (5):

$$m\left(\frac{d^2x_3}{dt^2}+\frac{d^2x_1}{dt^2}\right)+M_1\frac{d^2x_1}{dt^2}+F_e+k_1x_1+\beta_1\frac{dx_1}{dt}=0 \tag{4}$$

$$M_2\frac{d^2x_2}{dt^2}+\beta_2\frac{dx_2}{dt}+k_2x_2=F_e=k_3\left(x_3+x_1-\Delta x-x_2\right)+\beta_3\left(\frac{dx_3}{dt}+\frac{dx_1}{dt}-\frac{dx_2}{dt}\right) \tag{5}$$

where Δx is the initial distance between the rod and the stricken body, whose displacement is x_2. The flow proportional valves are modeled according to the ISO 6358, hence they are defined by a sonic conductance C and a critical ratio b. Being P_A and P_B respectively the upstream and downstream pressures, ρ_0 the air density at 25° C, the flow rate G is calculated with the following equations:

$$G=\rho_0P_AC \text{ for } 0<\frac{P_B}{P_A}\le b, \qquad G=\rho_0P_AC\sqrt{1-\left(\frac{P_B/P_A-b}{1-b}\right)^2} \text{ for } b<\frac{P_B}{P_A}\le 1 \tag{6}$$

The conductance C is almost proportional to the sectional area. Assuming that the static variation of the effective sectional area of the valve is linearly correlated to the voltage command V_{ref}, and given a first order dynamic behavior of the valve (time constant τ), the following simplified relation can be considered in which K_v is the static flow gain of the valve:

$$C=\frac{K_v}{1+\tau s}V_{ref}, \qquad K_v=\frac{C_{\max}}{V_{\max}} \tag{7}$$

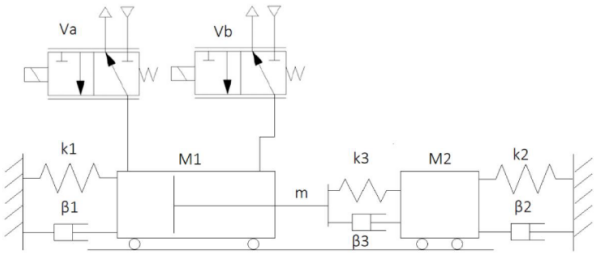

Fig. 3. Overall model of the perturbator and of the test bench.

Control logic. The control logic is sequential and has been developed in Stateflow® toolbox (The MathWorks, Inc., Natick, Massachusetts, USA). Four phases (1 – 4) have been designed as follows. While an external command triggered by the operator leads to the approach phase (1), the increase of the contact force measured by the load cell above a selected threshold generates the strike phase (2). A Proportional-Integral (PI) controller performing the actual control of the contact force has been implemented through the default blocks in Simulink®. The system allows the user to set customizable profiles, in terms of shape, amplitude and duration. For instance, the impulse can be set as a constant signal with a predefined level and duration, or as a ramp to reduce the dynamics of the force error signal. The fall of the reference force below a second threshold yields the return phase (3), which leads to the next idle state (4) after a timeout interval of 4 s.

Simulations and experimental trials. The parameters required to run the model have been obtained from the datasheets of the components selected for the experimental rig design. The unknown data, as the coefficients C and b of the valves, have been determined by experimental characterization of the respective components in laboratory. In order to avoid fast transients in the contact force, the behavior of the system for a smoother reference force profile with respect to the square wave used in [20] has been evaluated. The selected waveform (Fig. 4) is given by a sine wave plus a bias, with selected peak-to-peak amplitude and duration. The system has been tested in the following configurations:

A. carts of cylinder and stricken body fixed on the linear guide;
B. fixed cylinder cart and stricken body free to move;
C. both cylinder and stricken body carts free to move.

A first evaluation concerned the effect of the proportional k_p and integral k_i gains of the PI controller on the accuracy of the force tracking. Figure 4 presents the results of the model for different values of the proportional gain. The reference force profile had an amplitude of 50 N and lasted 300 ms, with impulse equal to 7,5 N·s. The default parameters selected for the stricken body mechanical impedance were M_2 = 10 kg, k_2 = 3000 N/m and β_2 = 1000 N·s/m. A first assessment of k_p was performed by iterative approach (i.e. Ziegler-Nichols), then it was manually tuned in order to get the most accurate result while avoiding oscillations in the control law.

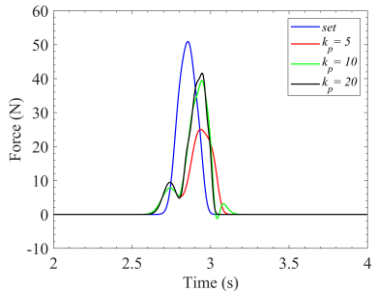

Fig. 4. Force tracking in the model for different values of the proportional gain.

The contribution of the integral gain k_i was not significant to improve the performance of the force tracking, therefore it was set to zero for the following simulations. The same result occurred in the experimental trials. Since there is no steady state for the controller to track, the force control accuracy during fast transients is likely to be by far more affected by the proportional gain, which determines the responsivity of the controller, rather than by the integral gain, which is generally required to avoid steady-state errors. The accuracy of the theoretical model has been validated by comparison with data from experimentation. To correctly match the results and to get a better approximation of the real system behavior, the proportional gain in the model had to be set about ten times greater than the one used in the experimentation. In this way, it was possible to get a better approximation of the real system behavior with the model. The results of this comparison for configurations A and B are presented in Fig.

5. The system in C configuration behaved similarly to B, therefore it has not been shown for sake of simplicity. Subsequently several force tracking tests for different configurations of the test bench have been performed. Results for configurations A and C are presented in Fig. 6.

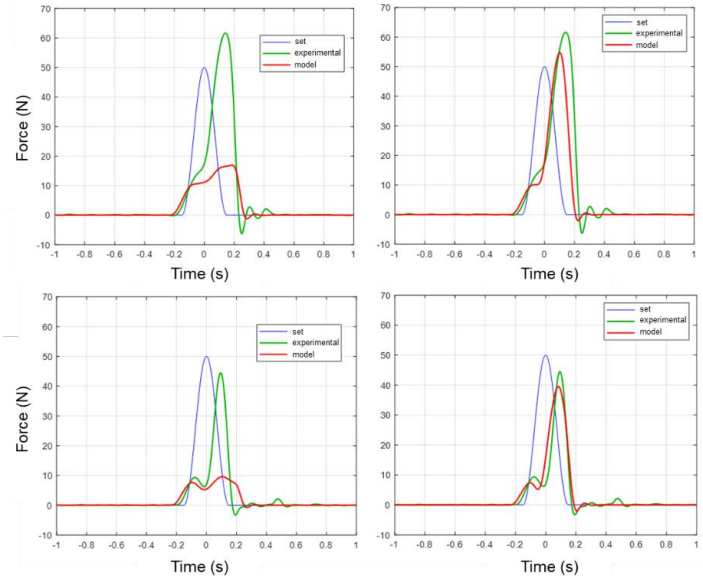

Fig. 5. Comparison between model and experimental data in different configurations (top: A; bottom: B) for different values of proportional gain (left: k_p = 1,5; right: k_p = 10).

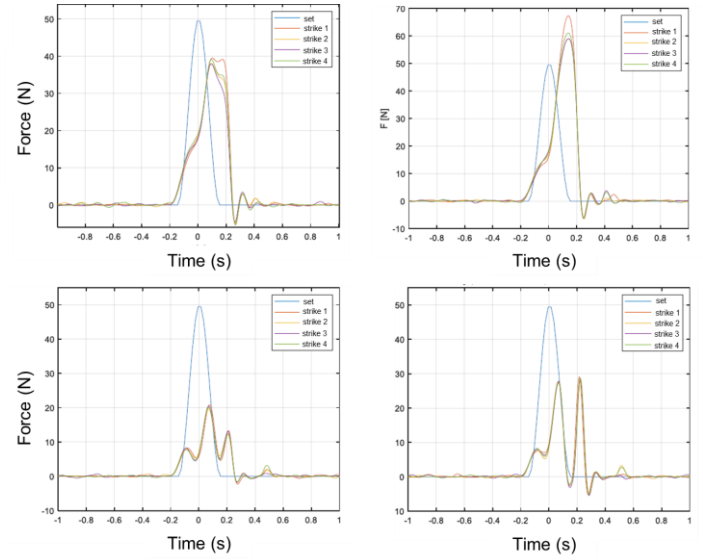

Fig. 6. Force tracking during experimental trials in different configurations (top: A; bottom: C) for different values of the proportional gain (left: k_p = 1; right: k_p = 1,5).

3 Results and discussion

Both simulations and experimental analyses showed that the system has limited accuracy and dynamics, and its performance deteriorates when low values of the controller gains are chosen. The comparison between the results of the model and of the experimentation (Fig. 5) shows good matching only when significantly higher controller gains are selected (in the model). However, the strong similarities highlighted demonstrate that the model has a sufficient level of accuracy and might be used to predict the behavior of the experimental system. The need for a scaling factor on the controller gains may be due to the lack of modelling of some aspects, as the pneumatic resistance related to the pipes or the friction forces acting on the carts of the linear guides. The most accurate results for force tracking have been collected for the configuration A (Fig. 6, top). For the default value of k_p = 1, the impulse value is about 7.3 N·s, close to the set value of 7.5 N·s. The duration of the impulse is about 70 ms longer than the reference one: the low dynamic performance is probably due to the limited time response of the valves selected. The relatively low slope of the first part of the contact force profile also depends on the compliance of the pad between the end striker of the perturbator and the target. The behavior of the system for k_p = 1,5 presents an overshoot of the contact force but allows for shorter lasting perturbations (about 352 ms). Regarding configurations B and C, the movement of the stricken body highly affects the accuracy of the force profile, producing a reduction in the increase of the force measured by the load cell (Fig. 6, bottom). The average duration is about 310 ms, thus quite close to the desired value. The increase of the controller gain allows for perturbations with higher peak level and still accurate durations. The value of the impulse, due to initial reduction of the contact force, is lower than the set value (about 4.4 N·s).

4 Conclusion

The realization of our target, i.e. of an Automatic Perturbator for postural analysis, requires the solution of several problems related to the mechanical interaction of the device with human subjects: the operator and the individual under test. In addition, the specific application poses very demanding performance, in terms of accuracy, dynamics, and ability to control not only the intensity of the contact force but also its impulse.

Our work demonstrated that the realization of a dedicated experimental bench, and its modeling, was a necessary step to achieve the result. The simulations of the system and the experimentation at the bench allowed for the optimization of the control parameters and highlighted the limits of the current prototype and the aspects that must be improved. In particular, the pneumatic actuation, although relatively not expensive and simple to be implemented, shows some drawbacks related to accuracy and dynamics. Improvements can be achieved by selecting more effective components, as low friction actuators and high-performance valves with reduced response time. The limited performance may also depend on the control logic, which is based only on the

feedback given by the load cell signal. In the future, a more robust control logic could be developed which will also incorporate the measurement of the actuator stroke, to improve the reliability of the system and to directly control the velocity of piston rod before impact. Concerning the model, it was shown to be able to match the experimental data with good accuracy, but improvements may be achieved by more accurate identification of some physical parameters like frictions and mechanical impedances.

References

1. Visser, J. E., et al: The clinical utility of posturography. Clinical Neurophysiology 119, 2424-2436 (2008).
2. Chen, B., et al: Role of point of application of perturbation in control of vertical posture. Exp Brain Res 235(11), 3449-3457 (2017).
3. Duncan, C. A., et al: Population Differences in Postural Response Strategy Associated with Exposure to a Novel Continuous Perturbation Stimuli: Would Dancers Have Better Balance on a Boat?. PLoS ONE 11(11), e0165735 (2016).
4. Piscitelli, D., et al: Anticipatory postural adjustments and anticipatory synergy adjustments: preparing to a postural perturbation with predictable and unpredictable direction. Exp Brain Res 235(3), 713-730 (2017).
5. Shahvarpour, A., et al: Trunk response to sudden forward perturbations – Effects of preload and sudden load magnitudes, posture and abdominal antagonistic activation. Journal of Electromyography and Kinesiology 24, 394-403 (2014).
6. Kamen, G., et al: An accelerometry-based system for the assessment of balance and postural sway. Gerontology 44(1), 40-45 (1998).
7. Moe-Nillsen, R., et al: Trunk accelerometry as a measure of balance control during quiet standing. Gait & Posture 16, 60-68 (2002).
8. Gandelman-Marton, R., Arlazoroff, A., Dvir, Z.: Ocular dominance and balance performance in healthy adults. Gait & Posture 31, 394-396 (2010).
9. Horak, F. B., Nashner, L. M., Diener, H. C.: Postural strategies associated with somatosensory and vestibular loss. Experimental brain research 82, 167-177 (1990).
10. Horak, F. B., Macpherson, J. M.: Postural orientation and equilibrium. In: Handbook of physiology, 253-292 (1996).
11. van der Kooij, H., et al.: Non-linear stimulus-response behavior of the human stance control system is predicted by optimization of a system with sensory and motor noise. J Comput Neurosci 30, 759-778 (2011).
12. van der Kooij, H., et al: An adaptive model of sensory integration in a dynamic environment applied to human stance control. Biological Cybernetics 84, 103-115 (2001).
13. Peterka, R. J.: Sensorimotor integration in human postural control. J Neurophysiol 88, 1097-1118 (2002).
14. van der Kooij, H., et al: Postural responses evoked by platform perturbations are dominated by continuous feedback. J Neurophysiol 98, 730-743 (2007).
15. Potocanac, Z., et al: A robotic system for delivering novel real-time, movement dependent perturbations. Gait & Posture 58, 386-389 (2017).
16. Ayena, J. C., et al: Home-based risk of falling assessment test using a closed-loop balance model. IEEE Transactions on Neural Systems and Rehabilitation Engineering 24(12), 1351-1362 (2016).
17. Martinelli, A. R., et al: Light touch modulates balance recovery following perturbation: from fast response to stance restabilization. Exp Brain Res 233(5), 1399-1408 (2015).

18. Chen, B., et al: Control of grip force and vertical posture while holding an object and being perturbed. Exp Brain Res 234, 3193-3201 (2016).
19. Davidson, B. S., et al: Neural control of posture during small magnitude perturbations: effects of aging and localized muscle fatigue. IEEE Transactions on Biomedical Engineering 58(6), 1546-1554 (2011).
20. Maffiodo, D., et al: Pneumo-tronic perturbator for the study of human postural responses. Advances in Intelligent Systems and Computing 980, 274-383 (2019).